EDGE ARTICLE

Check for updates

Visible-light-driven asymmetric aldol reaction of ketones and glycinates *via* synergistic Lewis acid/photoredox catalysis†

Jiuqi Tan, [ID] Longqing Yang, [ID] Hanyu Su, Yuntian Yang, Ziwei Zhong, [ID] Xiaoming Feng [ID] * and Xiaohua Liu [ID] *

Visible-light-driven direct asymmetric α-C(sp^3)–H bond functionalization of glycinate provides a direct and efficient route for the synthesis of diverse optically enriched α-amino acid derivatives. However, asymmetric coupling between glycinate radical species and ketones faces significant challenges, including competitive pathways, mutable intermediates, as well as congested stereogenic centers. Herein, we disclose the first example for the asymmetric photocatalytic synthesis of a diverse array of β-diaryl-β-hydroxy-α-amino acetate derivatives from glycinates and heteroaryl ketones through the synergistic catalysis of achiral iridium photoredox catalyst and chiral lanthanide Lewis acid catalysts. The enantioselective radical addition pathway is supported by spectroscopic experiments, control experiments and DFT calculations.
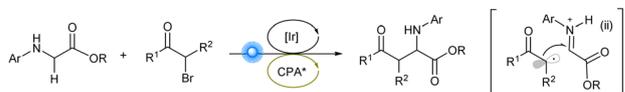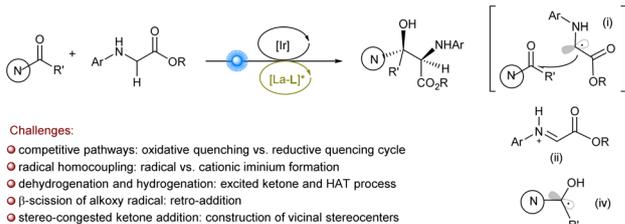
Introduction

Glycine is the only achiral proteinogenic α-amino acid, but the α-functionalization of the C(sp^3)–H bond of glycine derivatives provides a direct and efficient route for the synthesis of diverse natural or unnatural chiral α-amino acids and modified peptides.[1] Visible-light-driven α-C(sp^3)–H bond functionalization of glycinate has witnessed considerable developments benefiting from the harmonization of photoredox catalyst and/or metal complex/organocatalyst (Scheme 1a).[2] The general mechanistic profile involves the oxidation of glycine ester into amino radical cation, which triggers rapid α-deprotonation to yield a carbon-centered α-amino radical (i), then further oxidation into cationic iminium (ii).[3] Based on this strategy, a plethora of α-alkylation and α-arylation reactions of glycinate have been achieved using various alkyl sources and electron-rich aryls (Scheme 1a, path 1). Recently, the enantioselective variation was reported, which provides efficient access to optically enriched amino acid derivatives. Wang *et al.*[3e,3h] reported enantioconvergent cross-coupling between racemic α-bromo ketones and *N*-substituted glycine esters by a cooperative photoredox/Brønsted acid catalysis (Scheme 1b). Xu *et al.* realized the enantioselective alkylation of quinolinyl-preinstalled glycinate derivative using *N*-hydroxyphthalimide (NHP) esters as the

alkyl radical sources enabled by photoinduced chiral copper complexes.[4] However, there are sporadic reports related to the addition or coupling with unsaturated compounds (Scheme 1a, path 2), such as carbonyl compounds reported by Xiao *et al.*,[5a] azo compounds by Fu *et al.*,[5b] or phenylpropyne by Breit *et al.*,[5c]

(a) Visible-light-driven α-C(sp^3)-H bond functionalization of glycine derivatives
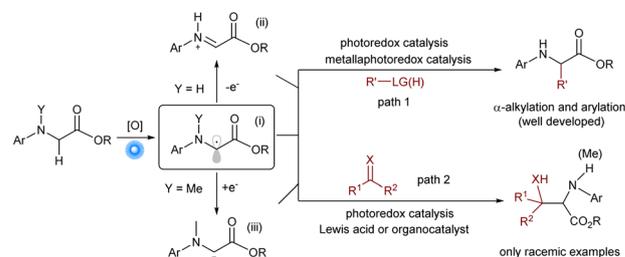
(b) Enantioconvergent radical coupling reaction by dual Brønsted acid/photoredox catalysis[3e,3h]

(c) Enantioselective radical addition reaction by Lewis acid/photoredox catalysis (this work)

Challenges:
- competitive pathways: oxidative quenching vs. reductive quenching cycle
- radical homocoupling: radical vs. cationic iminium formation
- dehydrogenation and hydrogenation: excited ketone and HAT process
- β-scission of alkoxy radical: retro-addition
- stereo-congested ketone addition: construction of vicinal stereocenters

Scheme 1 Visible light-driven α-C(sp^3)–H bond functionalization of glycinates.

Key Laboratory of Green Chemistry & Technology, Ministry of Education, College of Chemistry, Sichuan University, Chengdu 610064, P. R. China. E-mail: xmfeng@scu.edu.cn; liuxh@scu.edu.cn

which could serve as complementary approaches to the α-C(sp³)–H bond functionalization of glycinate. Moreover, König et al.[6] utilized 3DPA2FBN as the photocatalyst to trigger the formation of carbanion intermediate (iii) bearing an exogenous alkylamine substitution, leading to the addition into carbonyl compounds.

β-Hydroxy-α-amino acids are a class of molecules commonly found in polypeptide natural products and pharmaceuticals.[7] The direct aldol reaction of glycinates represents an intriguing and straightforward strategy.[8,9] Zhao et al. realized biomimetic aldol reaction of trifluoromethyl ketones[9f,g] and aldehydes[9h] by carbonyl catalysis. The enantioselective α-C(sp³)–H functionalization of glycinate to general ketones remains elusive. Intrigued by visible-light-driven radical cross-coupling between glycinates and diaryl ketones,[5a,6] we wish to achieve the more challenging enantioselective synthesis of β-diaryl-β-hydroxyl-α-amino acids via this approach.

There are several challenges for the target process (Scheme 1c). The use of photoredox catalysts is imperative but both glycinate and ketone can perform the SET process, which may cause competitive catalytic cycles: reductive quenching or oxidative quenching cycle.[10] The excessive oxidation of glycinate into cationic iminium (ii) is disadvantageous to the coupling with ketone, enhancing the formation of the diamine byproduct. The conjugated system of diaryl ketones leads to the excited species via the direct absorption of visible light or energy transfer from photocatalysts,[11–13] and the formed ketyl radical (iv) gives rise to the hydrogenation of ketone and dehydrogenation of glycinate. In addition, the addition to ketones results in the construction of vicinal stereo-congested centers, including a quaternary carbon center, which is one of the synthetic challenges in asymmetric catalysis. In addition, the alkoxy radical intermediate might undergo β-scission, leading to the decomposition of the product.[14] The merging of a photoredox catalyst and a chiral catalyst for synergistic catalysis would provide an important platform, which could not only control the formation of the radical species to minimize undesired radical species but also guide the facial approach of the two reactive species. Herein, we disclosed a new synergistic catalysis by the combination of an Ir(III)-based photoredox catalyst and chiral lanthanide catalyst of N,N'-dioxide ligands developed by our group for the purpose.[15,16] The first example for the visible light-driven asymmetric α-C(sp³)–H bond functionalization of glycinate for the synthesis of β-quaternary-stereocentric serine derivatives was achieved (Scheme 1c).

Results and discussion

Initially, we chose phenyl(pyridin-2-yl)methanone A1 and ethyl phenylglycine B1 as the model substrates to identify the optimal catalytic system (Table 1 and see ESI† for details). The screening of a number of metal salts combined with chiral N,N'-dioxide L₃-RaPr₂ in the presence of photocatalyst [Ir1] and DMAP as the base at room temperature revealed that lanthanide salts with larger ion radii showed higher enantioselectivity. We found that La(OTf)₃ could give product C1 excellent ee value for two diastereomers and moderate yield (Table 1, entry 1). The use of

organic photocatalyst 4CzIPN (entry 2) or [Ir2] (entry 3) gave the product with slightly increased diastereoselectivity, although the yield dropped. Using the ligand L₃-RaPr₃ with increased steric hindrance at the amide subunits gave rise to the product with somewhat higher diastereoselectivity (entry 4). The yield of amino alcohol C1 is not good due to the strongly competitive reactions, which led to the generation of homo-coupling F and oxidated imine G from B1 and also the reduced byproduct H from A1. Later, when the transformation was carried out with weakened irradiation light (entry 5), decreased reaction temperature (entry 6), and lower amount of [Ir2] (entry 7) within less reaction time (10 hours; entry 8), the desired amino alcohol C1 could be isolated in a gradually increased yield as a result of minimizing the formation of byproducts and avoiding the decomposition of the product. In these conditions, product C1 could be isolated in 66% yield, with 98% and 92% ee for each diastereomers once the amount of glycinate increased to three equivalents (entry 9). Fortunately, the reaction can be further enhanced by the addition of 30 mol% of sodium tetrakis[3,5-bis(trifluoromethyl)phenyl]borate (NaBArF₄), resulting in a 93% NMR yield of the product and 84% isolated yield (entry 10). This result might contribute to the counteracting ion exchange with lanthanide catalyst and [Ir2] or the stabilization of the alkoxy radical intermediate (see ESI† for details). The concentration did not considerably affect the reaction results (entry 11). Considering environmental friendliness and economic efficiency, we chose a minimal quantity of the solvent. The homo-coupling product F was obtained in about 5% yield and the imine G was detected in 7% yield. In addition, the alcohol H was detected in less than 4% yield in this case. Finally, the optimal conditions (entry 11) giving the amino alcohol C1 in the best selectivity and isolated yield (84% yield, 68:32 dr, with 98% and 92% ee for each isomer) involved 0.5 mol% of [Ir2], chiral La(OTf)₃/L₃-RaPr₃ catalyst, and DMAP in THF (0.2 M) under the irradiation of visible light (460 nm, 2 W) at −30 °C after 10 h. The system was sensitive to air but water and other protonic additives were tolerable (see ESI† for details). We also tested several other chiral ligands, such as bisoxazoline and phosphine ligands, as well as chiral phosphoric acid organocatalysts, but the stereoselectivity was poor (see ESI† for details). The comparison reaction in the presence of only [Ir2] and DMAP generated the racemic diastereomers in 19% yield, and ketone was recovered in 56% yield (entry 12 vs. entry 8), highlighting the acceleration of lanthanum catalyst. Note that the mixture of ketone A1 and glycinate B1 in the presence of chiral lanthanum catalyst could afford the product upon direct irradiation with 400 nm light without an additional photocatalyst, and the amino alcohol was isolated in 38% yield with maintained enantioselectivity (entry 13). It manifested that this addition reaction could be performed via different pathways depending on the photocatalyst, ketone, and light energy as well.

With the optimal reaction conditions (Table 1, entry 11) established, the substrate scope with respect to glycinates was investigated. As shown in Scheme 2, phenylglycinates with varied ester group regardless of the steric hindrance reacted with ketone A1 smoothly, providing the desired serine

Table 1 Optimization of the reaction conditions[a]
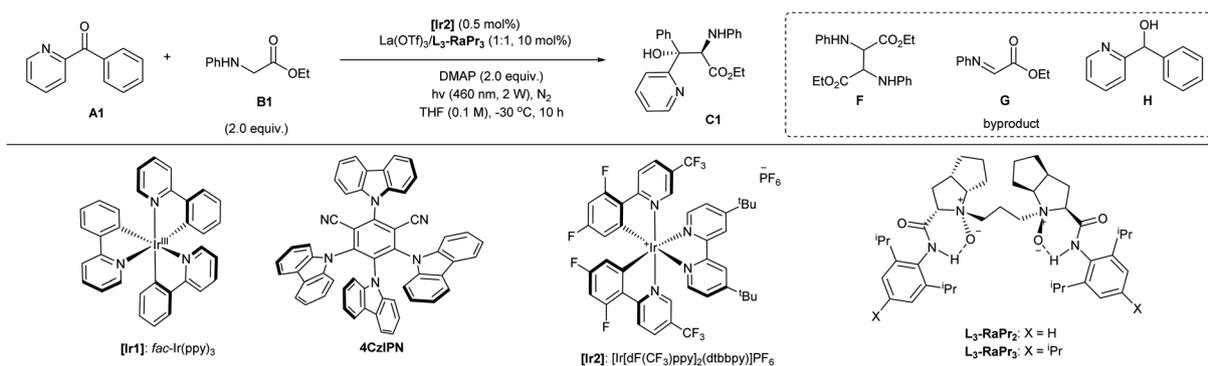
| Entry	Condition variation	Yield[b] (%)	ee[c] (%)	dr[c]
1	**L$_3$-RaPr$_2$/[Ir1]** (2 mol%)/5 W/r.t./24 h	35	99/91	52 : 48
2	**L$_3$-RaPr$_2$/4CzIPN** (2 mol%)/5 W/r.t./24 h	22	98/92	60 : 40
3	**L$_3$-RaPr$_2$/[Ir2]** (2 mol%)/5 W/r.t./24 h	10	99/91	60 : 40
4	**[Ir2]** (2 mol%)/5 W/r.t./24 h	16	93/90	66 : 34
5	**[Ir2]** (2 mol%)/r.t./24 h	30	95/93	66 : 34
6	**[Ir2]** (2 mol%)/24 h	36	95/91	72 : 28
7	24 h	51	95/92	68 : 32
8	—	60	98/92	70 : 30
9	**B1** (3.0 equiv.)	66	98/92	66 : 34
10	**B1** (3.0 equiv.)/NaBAr$^F_4$ (30 mol%)	85 (93)	98/93	68 : 32
11	**B1** (3.0 equiv.)/NaBAr$^F_4$ (30 mol%)/THF (0.5 mL)	84 (93)	98/92	68 : 32
12	w/o **L$_3$-RaPr$_3$**/La(OTf)$_3$	19	—/—	50 : 50
13	w/o **[Ir2]**/400 nm/15 °C/24 h	38	98/93	58 : 42

[a] Unless otherwise noted, all reactions were carried out with **A1** (0.1 mmol), **B1** (2.0 equiv.), La(OTf)$_3$/**L$_3$-RaPr$_3$** (1:1, 10 mol%), DMAP (0.2 mmol), **[Ir2]** (0.5 mol%) in THF (1.0 mL) at −30 °C upon irradiation with LEDs (460 nm, 2 W) under nitrogen for 10 hours. [b] Total isolated yield of two diastereoisomers, and the data in the parentheses referred to the ^{1}H NMR yield with dibromomethane as the internal standard. [c] ee and dr values were determined by HPLC analysis on a chiral stationary phase. DMAP = 4-dimethylaminopyridine. THF = tetrahydrofuran. r.t. = room temperature.

derivatives **C1–C4** in good yield (77–84%) and excellent levels of enantioselectivity for each diastereomer (98–99% ee for major diastereomer, 91–98% ee for the minor one). The *para*-tertbutyl group introduced at the *N*-aryl substitution slightly raised the diastereoselectivity (**C5–C6**), and the absolute configuration of the major isomer of the product **C5** was determined to be (2*R*,3*R*) by X-ray crystallography analysis.[17] Ether glycinates bearing a series of substituted aryl groups as *N*-protection groups could be tolerated well. It revealed that *ortho*-substituents had a greater effect on both the yield and the stereoselectivity due to the steric hindrance (**C7–C8**); however, various substitutions at the *meta*- and *para*-position had no obvious influence on the enantioselectivity of each diastereomers (**C9–C27**; 91–99% ee for major diastereomer, and 82–93% ee for the minor one). The yields were satisfactory with *para*-cyano group (**C21**) as an exception, probably because its high oxidation potential is unfavorable to the photo-reductive quenching of **[Ir2]**. Notably, several functional groups, such as alkenyl (**C22**), alkynyl (**C23**), acyl (**C24**), ester (**C25**), boron ester group (**C26**), were compatible in the transformation. 1-Naphthyl (**C28**) and 2-naphthyl substitutions (**C29**) were competent in the reaction, but the former showed lower outcome as a result of steric hindrance. *N*-PMP-containing product **C30** was isolated in 40%

yield because of the thermodynamic instability in column chromatography purification. Moreover, this approach could be applied to late-stage modification (**C31–C34**), involving the introduction of alcohols to glycine as ester groups or peptide as the amide substitution.

Subsequently, we turned our attention to the variation of ketones. As shown in Scheme 3, a series of 2-pyridine-based diaryl ketones bearing electron-deficient or -rich substitutions on the *meta*- or *para*-position of the phenyl ring performed well, and they delivered the corresponding adducts **C35–C46** in moderate to good yields (66–81%) and excellent enantioselectivities (91–99% ee for the major diastereomer and 71–98% ee for the minor one), and the diastereoselectivity (up to 90 : 10 dr) was higher when there was a *para*-substituted phenyl group. *Ortho*-substitutes were not eligible to the addition, which might be due to the spatial congestion hindering the addition of radical species (see ESI† for details). Pyridin-2-yl(pyridin-4-yl) methanone delivered the related product **C47** in 70% yield with good enantioselectivity (93%/87% ee) and 72:28 dr. Substitution at the C2 or C3-position of the pyridine subunit (**C48–C51**) could be compatible, but the C4-bromo substituted one led to the formation of **C52** with decreased enantioselectivity, especially for the minor isomer. The 2-pyridinyl group
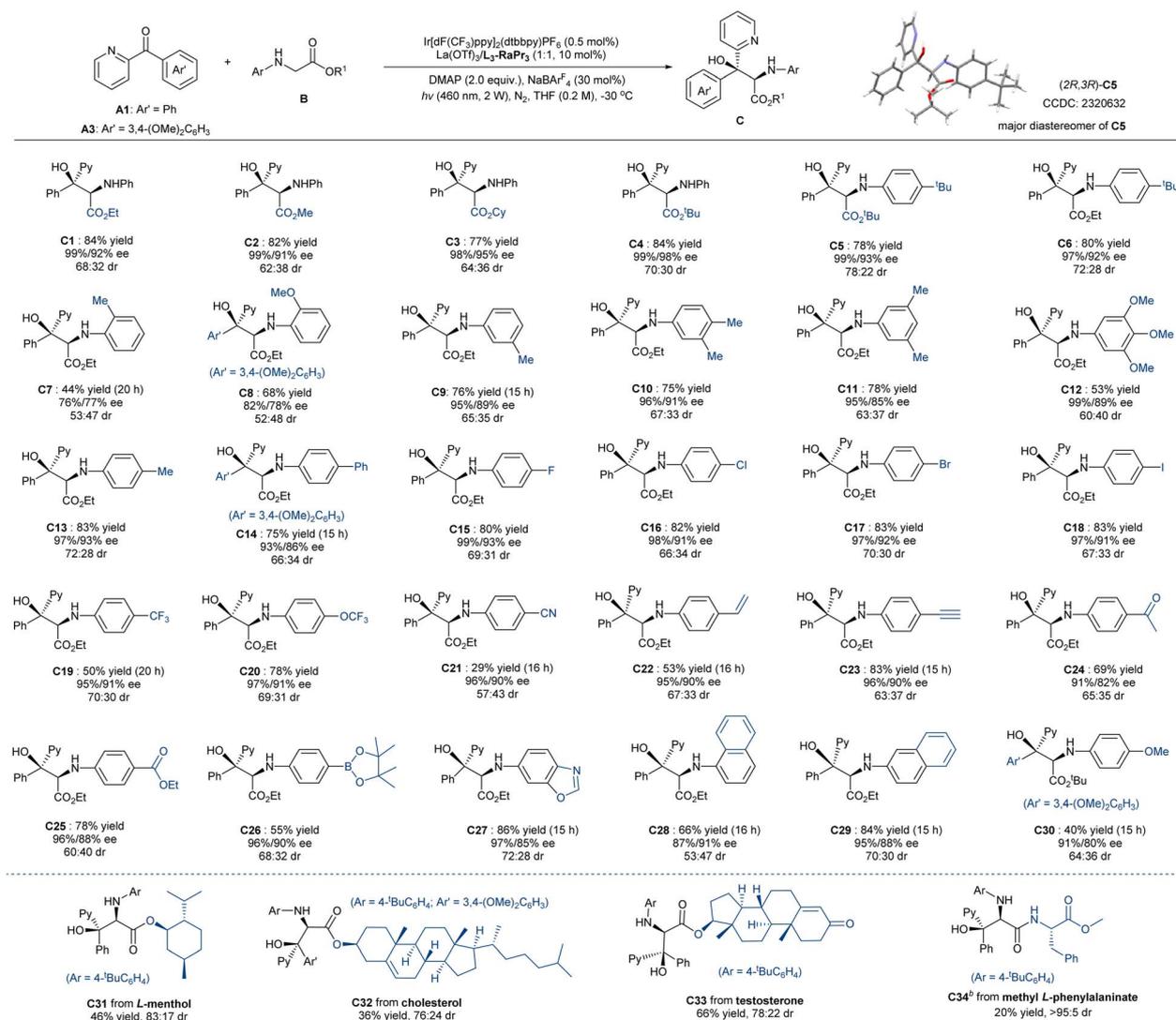
Scheme 2 Substrate scope of N-aryl glycinate derivatives.[a] Unless otherwise noted, all reactions were carried out with **A1** or **A3** (0.1 mmol), **B** (3.0 equiv.), La(OTf)$_3$/**L$_3$-RaPr$_3$** (1:1, 10 mol%), DMAP (0.2 mmol), [**Ir2**] (0.5 mol%), NaBAr$^F_4$ (30 mol%) in THF (0.2 M) at −30 °C upon irradiation with LEDs (460 nm, 2 W) under nitrogen for 10 hours. Total isolated yield of two diastereoisomers. ee values were determined by HPLC or UPC^2 analysis on a chiral stationary phase. dr value was determined by ^{1}H NMR.[b] **4CzIPN** (2 mol%), at 20 °C for 20 h.

of the ketone could be changed into the 3-isoquinolinyl (**C53**) or 2-pyrimidinyl group (**C54**) without diminishing the reactivity and enantioselectivity. In contrast, the addition of di(pyridin-2-yl)methanone yielded the product **C55** with a poor ee value (20% ee), indicating that the diastereoselectivities of the unsymmetric ketones originate from the facially selective approach of glycinate and that the tertiary alcohol centers of the two isomers are likely to be identical in other cases. Additionally, 1-(pyridin-2-yl)ethan-1-one (**C56**) and benzothiazolphenone (**C58**) worked well despite there being a slight decrease in the reactivity (61–67% yield) and enantioselectivity. The reaction of cyclopropyl(pyridin-2-yl)methanone afforded the product **C57** in moderate yield without ring-opening, manifesting that the addition process did not involve the ketyl radical intermediate.

As shown in Scheme 4a, the reaction of ketone **A1** at the 4 mmol scale with glycinate **B5** performed well under the

optimized reaction conditions, and the gram-scale synthesis of **C5** gave 80% yield (1.42 g) with 99%/93% ee and 78:22 dr. Using the enantiomer of the ligand **L$_3$-RaPr$_3$** instead, *ent*-**C5** was delivered with comparable results (see ESI† for details). After recrystallization, nearly optically pure **C5** (99% ee, >95:5 dr) was obtained, which could be readily reduced into the useful 2-amino-1,3-diol[18] **D1** by diisobutylaluminium hydride (DIBAL-H) or be transformed into oxazolidinone **D2** in moderate yield without the erosion of stereoselectivity after the treatment with triphosgene.

To glean insights into the overall mechanism, some spectroscopic studies and control experiments were conducted (Scheme 4 and ESI†). UV-vis absorption spectroscopy analysis suggested that the main light-absorbing species is the iridium photocatalyst rather than ketone **A1** or glycine ester **B5** under the irradiation at 460 nm (see ESI† for details). Stern–Volmer
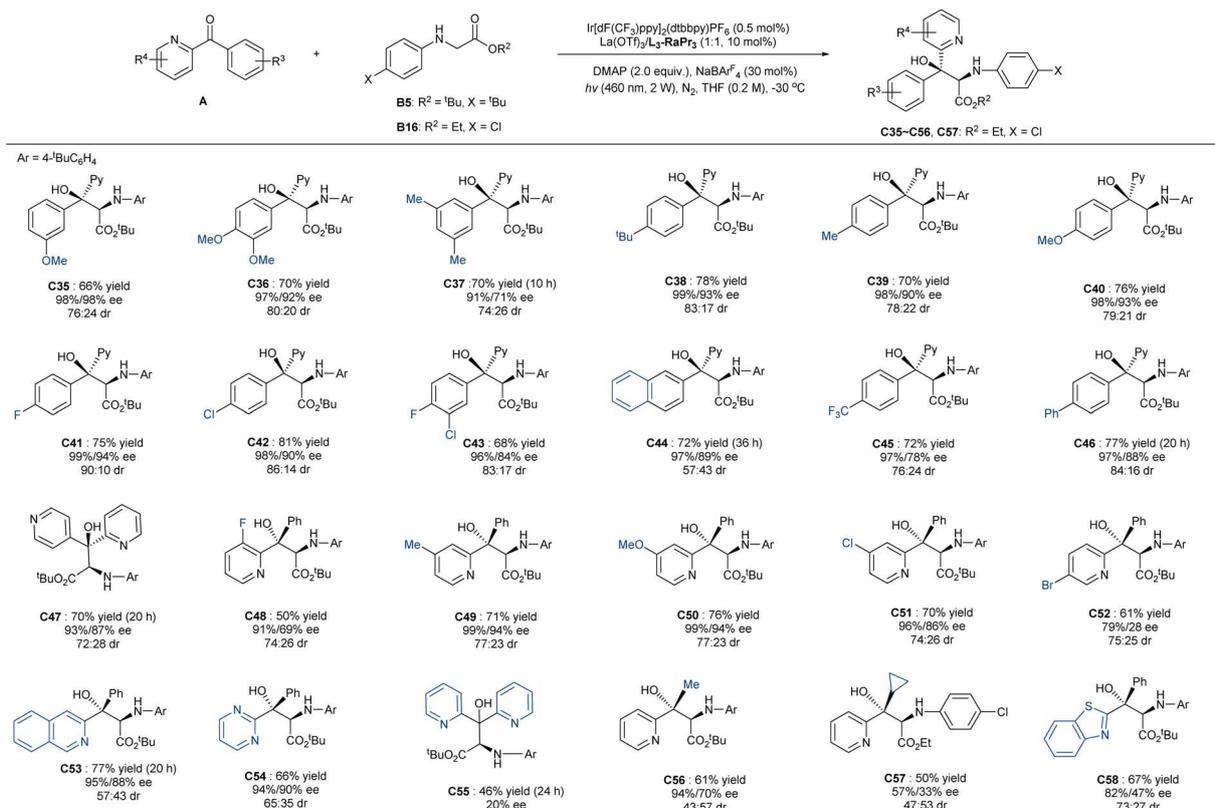
Scheme 3 Substrate scope of ketones. [a] Unless otherwise noted, all reactions were carried out with **A** (0.1 mmol), **B5** or **B16** (3.0 equiv.), La(OTf)₃/**L₃-RaPr₃** (1:1, 10 mol%), DMAP (0.2 mmol), **[Ir2]** (0.5 mol%), NaBArᶠ₄ (30 mol%) in THF (0.2 M) at −30 °C upon irradiation with LEDs (460 nm, 2 W) under nitrogen for 15 hours. Total isolated yield of two diastereoisomers. ee values were determined by HPLC or UPC² analysis on a chiral stationary phase. dr value was determined by ¹H NMR.

fluorescence quenching studies (Scheme 4b) showed that the excited photocatalyst **[Ir2]** ($*E^{red}$ ($*Ir^{III}/Ir^{II}$) = +1.21 V *vs.* SCE)[10a] could be quenched by both glycine ester **B5** ($E_{p/2}^{ox}$ = +0.85 V *vs.* SCE) and **A1** or La(ɪɪɪ)-bonded **A1**, but the plot manifested that the quenching by the former is much stronger than that by the ketone, indicating a more favorable reductive quenching cycle. Furthermore, electrochemical measurement (Scheme 4c, all *vs.* SCE in MeCN) suggested that ketone **A1** had lower reductive potential [$E_{p/2}^{red}$ (**A1/A1**$^{·−}$) = −1.6 V], which shifted to about −0.82 V in the presence of La(OTf)₃, but the current intensity was low. Although the photoexcited state *Ir(ɪɪɪ) [$*E^{ox}$ (Ir^{IV}/*Ir^{III}) = −0.89 V] or Ir(ɪɪ) [$E_{1/2}$ = −1.37 V][10a] might serve as a reductant to reduce Lewis acid-activated carbonyl **A1** to afford the corresponding ketyl radical, this process will not dominate during the transformation in view of both the Stern–Volmer quenching experiments and radical clock experiments (see ESI† for details). This trend differed from the racemic reaction of benzophenone promoted by **[Ir1]**/LiBF₄ cooperation catalysis in Xiao's report,[5a] in which the generation of the ketyl radical species of ketone *via* the reduction of Ir(ɪɪɪ)* was proposed. The light on/off experiment between **A1** and **B5** indicated that continuous irradiation was essential for the formation of the product, and the quantum yield was found to be 0.022, excluding a radical chain-dominated process.

Next, radical trapping experiment was conducted (Scheme 4d) and it displayed that the addition process was completely inhibited by 2,2,6,6-tetramethylpiperidine-1-oxyl (TEMPO), and the radical coupling adduct **E1** was detected by high resolution mass spectrometry (HRMS), along with piperi-din-1-ol **E2** *via* the HAT process in 11% isolated yield (Scheme 4d). In connection with the detected byproducts **F** and **G** (Table 1), it is hypothesized that the reaction process involves reactive α-amino carbon radical species (see ESI† for details). Moreover, when imine **G** was added into the reaction system (Scheme 4e), the major coupling product is related to the glycinate **B15**, confirming that the formation of the ketyl radical is the least as stated above. A primary kinetic isotope effect (KIE) was obtained by parallel (KIE = 3.0) and competition reactions (KIE = 4.0), which indicated that the C–H cleavage of glycinate has a significant contribution to the rate-determining step (Scheme 4f).

In addition, a linear relationship between the enantiomeric excess of ligand **L₃-RaPr₃** and the enantiomeric excess of product **C50** was observed, indicating that the metal salt and the chiral N,N'-dioxide ligand were coordinated in a 1:1 ratio without catalyst aggregation in the active catalytic species (see the ESI† for details).

Based on the above analysis, a possible dominant mechanism is proposed in Fig. 1a to rationalize the synergistic catalysis. The reaction is initiated with excited *[Ir^{III}] photocatalyst
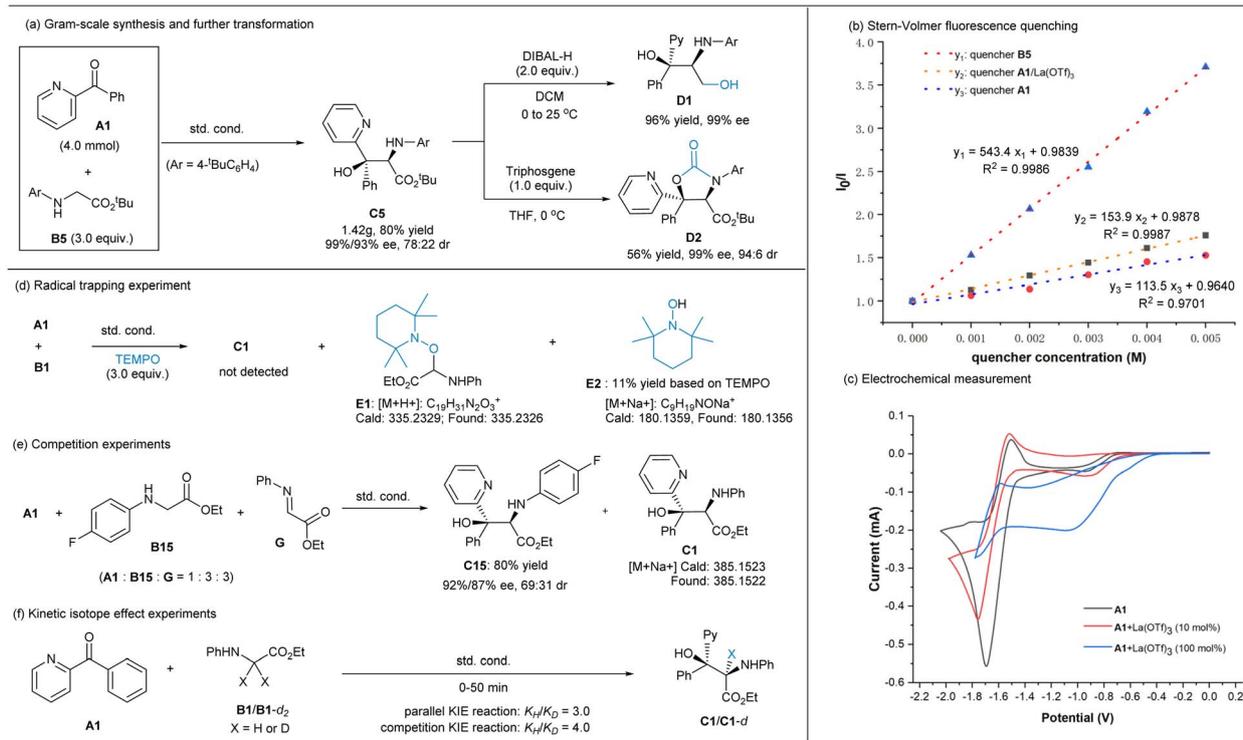
Scheme 4 Synthetic application and mechanistic investigation.

oxidation and DMAP deprotonation sequence of glycine ester **B1** into α-amino radical **Int I**. Subsequently, the radical **Int I** rapidly adds to the chiral Lewis acid bidentate-bonded ketone complex (**A1/[La]***), generating alkoxy radical species **Int II** bonded by the chiral Lewis acid catalyst (path a). Otherwise, the simple alkoxy radical would readily show β-scission[14] to recover the ketone and **Int I**. However, DFT calculation revealed the stabilization of the alkoxy radical by the chiral catalyst or proton

(see ESI† for details). We propose that after the release of the chiral Lewis acid catalyst, the protonated **Int III** of the alkoxy radical shows the reductive process with [Ir^{II}] species (E^{red} (Ir^{III}/Ir^{II}) = −1.37 V vs. SCE)[10a] to form the product, along with the regeneration of the [Ir^{III}] photocatalyst. During this process, the α-amino radical **Int I** may undergo further oxidation to yield the imine byproduct or the formal homocoupling diamine byproduct. On the other hand, in the absence of the
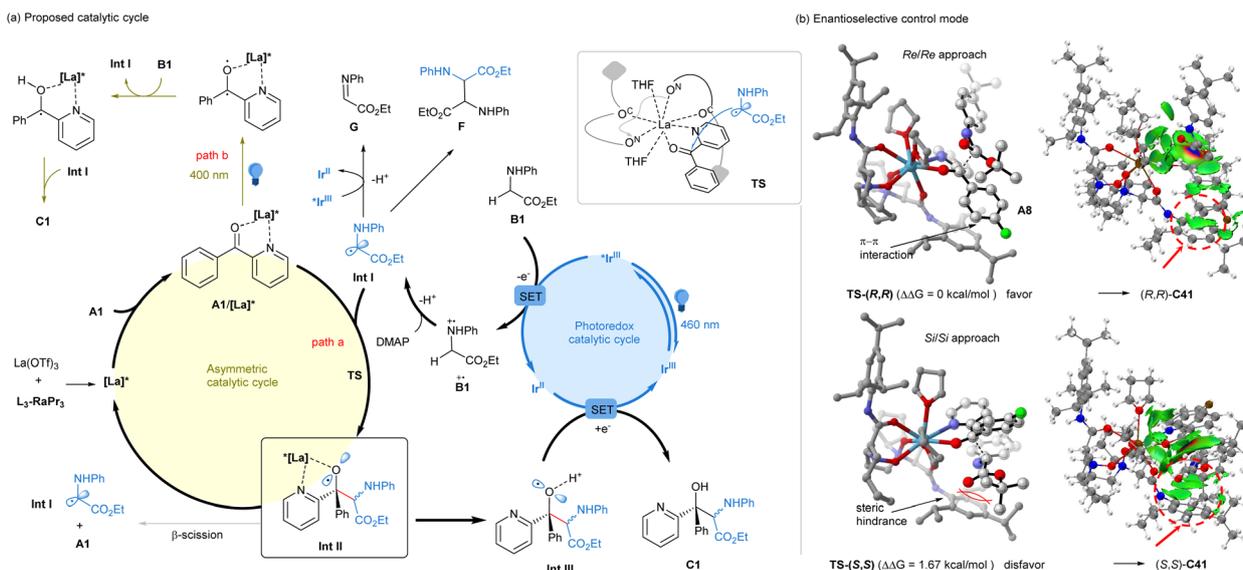

Fig. 1 Proposed catalytic cycle.

photocatalyst, the chiral Lewis bonded ketone could be excited at 400 nm irradiation,[16c,d] which acts as a strong oxidant to transfer glycinate into the related radical species **Int I** or imine intermediate (path b). Following radical–radical cross-coupling or addition, the desired product could also be generated.

To elucidate the underlying cause of the enantioselectivity induced by the N,N'-dioxide ligand, we carried out DFT calculations employing the chiral La(OTf)$_3$/**L$_3$-RaPr$_3$** complex in the enantio-determining step of the intermediate **Int II** (see ESI† for details).[19] As depicted in Fig. 1b, the eight coordination sites of La(III) were saturated by **L$_3$-RaPr$_3$**, THF and bidentate ketone **A8**. Two facial selective pathways during the radical addition process were to generate the major diastereomer **Int II**: (Re/Re) approach *vs.* the (Si/Si) approach between the ketone and radical **Int I**. The energy of the transition state **TS-(R,R)** in the (Re/Re) manner is 1.67 kcal lower than that of **TS-(S,S)**. From the perspective of Boltzmann distribution, this energy difference corresponds to approximately 95% ee to generate **C41**, which is consistent with the experimental observations. The IGMH weak interaction analysis[20] clearly reveals the reasons behind this difference. There is a weak π–π interaction between the aryl groups of ketone **A8** and one aniline unit of the N,N'-dioxide ligand in **TS-(R,R)**. However, there is steric hindrance between the ester group of radical **Int I** and the lower right aryl group of the ligand in **TS-(S,S)**.

Conclusions

The synergistic catalysis of the iridium photoredox catalyst and the chiral lanthanide complex of N,N'-dioxide enables the direct asymmetric α-C(sp^3)–H bond functionalization of glycinates with ketones. This effective protocol allows for the straightforward preparation of a wide range of valuable enantioenriched unnatural β-quaternary stereocentric serine derivatives with excellent enantioselectivities for both the diastereomers. The cooperation of the chiral Lewis acid catalyst not only harmonized the enantioselective radical addition step but also stabilized the alkoxy radical species before reduction. The multiplicative enhancement minimized the competitive byproduct formation and overwhelming racemic background reaction. This cooperative catalytic system holds promise for the development of a wide array of asymmetric catalytic direct α-C(sp^3)–H bond functionalizations through visible light-driven pathways.

Data availability

Further details of the experimental procedure, ^{1}H, ^{13}C{^{1}H} and ^{19}F{^{1}H} NMR, HPLC spectra, X-ray crystallographic data for **C5** are available in the ESI.†

Author contributions

J. Q. T. performed experiments and prepared the ESI† and paper. L. Q. Y. conducted the DFT calculation. Y. T. Y. repeated some experiments. H. Y. S. and Z. W. Z. participated in structure characterization and discussion. X. H. L. helped with modifying the paper and ESI.† X. H. L. and X. M. F. conceived and directed the project.

Conflicts of interest

There are no conflicts to declare.

Notes and references

1 (a) V. A. Soloshonok and K. Izawa, *Asymmetric Synthesis and Application of a-Amino Acids*, Oxford University Press, Washington, 2009; (b) A. B. Hughes, Amino Acids, Peptides and Proteins in Organic Chemistry, *Analysis and Function of Amino Acids and Peptides*, Wiley, Hoboken, 2013.

2 For selected reviews on α-C(sp^3)–H bond functionalization of glycinate:(a) T. A. King, J. M. Kandemir, S. J. Walsh and D. R. Spring, *Chem. Soc. Rev.*, 2021, **50**, 39–57; (b) M. Hari Babu and J. Sim, *Eur. J. Org Chem.*, 2022, e202200859; (c) Y. Tian, X. B. Bu, Y. R. Chen, L. H. Wang, J. N. E, J. Zeng, H. Xu, A. H. Han, X. B. Yang and Z. Zhao, *Catalysts*, 2023, **13**, 1502; (d) C. Wang, R. P. Qi, R. Wang and Z. Q. Xu, *Acc. Chem. Res.*, 2023, **56**, 2110–2125; (e) G. Q. Xu, W. D. Wang and P. F. Xu, *J. Am. Chem. Soc.*, 2024, **146**, 1209–1223; (f) W. Wang, L. M. Xuan, Q. L. Chen, R. D. Fan, F. Zhao, J. H. Dong, H. F. Wang, Q. J. Yan, H. Zhou and F. E. Chen, *J. Am. Chem. Soc.*, 2024, **146**, 6307–6316.

3 For selected examples of cationic iminium:(a) X. W. Gao, Q. Y. Meng, J. X. Li, J. J. Zhong, T. Lei, X. B. Li, C. H. Tung and L. Z. Wu, *ACS Catal.*, 2015, **5**, 2391–2396; (b) Y. Zhang, S. L. Li, Y. Zhu, X. R. Yang, H. Zhou and Y. Li, *J. Org. Chem.*, 2020, **85**, 6261–6270; (c) Z. Q. Zhu, D. Guo, J. L. Ji, X. Zhu, J. Tang, Z. B. Xie and Z. G. Le, *J. Org. Chem.*, 2020, **85**, 15062–15071; (d) H. Zhao and D. Leonori, *Angew. Chem., Int. Ed.*, 2021, **60**, 7669–7674; (e) C. Che, Y. N. Li, X. Cheng, Y. N. Lu and C. J. Wang, *Angew. Chem., Int. Ed.*, 2021, **60**, 4698–4704; (f) M. H. Babu and J. Sim, *Eur. J. Org Chem.*, 2022, e2022008591; (g) C. H. Jiang, X. F. Sha, C. Ni, W. Qin, X. J. Zhu, S. Wang, X. Li and H. F. Lu, *J. Org. Chem.*, 2022, **87**, 8744–8751; (h) C. Che, Y. N. Lu and C. J. Wang, *J. Am. Chem. Soc.*, 2023, **145**, 2779–2786; (i) S. T. Wang, Y. J. Ye, H. L. Shen, J. L. Liu, Z. Liu, Z. G. Jiang, J. Q. Lei and Y. Zhang, *Org. Biomol. Chem.*, 2023, **21**, 8364–8371; (j) C. Che, Y.-N. Lu, T. Fang, G.-J. Zhen, X. T. Qi and C.-J. Wang, *ACS Cent. Sci.*, 2024, DOI: **10.1021/acscentsci.4c00970**.

4 (a) R. P. Qi, C. Wang, Y. M. Huo, H. L. Chai, H. Y. Wang, Z. J. Ma, L. Y. Liu, R. Wang and Z. Q. Xu, *J. Am. Chem. Soc.*, 2021, **143**, 12777–12783; (b) R. Qi, C. Wang, Z. Ma,

H. Wang, Q. Chen, L. Liu, D. Pan, X. Ren, R. Wang and Z. Q. Xu, *Angew. Chem., Int. Ed.*, 2022, **61**, e202200822.

5 (*a*) W. Ding, L. Q. Lu, J. Liu, D. Liu, H. T. Song and W. J. Xiao, *J. Org. Chem.*, 2016, **81**, 7237–7243; (*b*) G. Z. Wang, D. G. Liu, M. T. Liua and Y. Fu, *Green Chem.*, 2021, **23**, 5082–5087; (*c*) J. Zheng and B. Breit, *Angew. Chem., Int. Ed.*, 2019, **58**, 3392–3397.

6 K. Murugesan, K. Donabauer, R. Narobe, V. Derdau, A. Bauer and B. König, *ACS Catal.*, 2022, **12**, 3974–3984.

7 For selected examples on bioactivites of β-hydroxy-α-amino acids:(*a*) M. A. T. Blaskovich, *J. Med. Chem.*, 2016, **59**, 10807–10836; (*b*) U. Galm, E. W. Pienkowski, L. Y. Wang, N. P. George, T. J. Oh, F. Yi, M. F. Tao, J. M. Coughlinc and B. Shen, *Mol. BioSyst.*, 2009, **5**, 77–90; (*c*) H. Hashizume, K. Iijima, K. Yamashita, T. Kimura, S. Wada, R. Sawa and M. Igarashi, *J. Antibiot.*, 2018, **71**, 129–134; (*d*) C. J. Mathias, *Clin. Auton. Res.*, 2008, **18**, 25–29; (*e*) D. A. Wirtz, K. C. Ludwi, M. Arts, C. E. Marx, S. Krannich, P. Barac, S. Kehraus, M. Josten, B. Henrichfreise, A. Müller, G. M. König, A. J. Peoples, A. Nitti, A. L. Spoering, L. L. Ling, K. Lewis, M. Crüsemann and T. Schneider, *Angew. Chem., Int. Ed.*, 2021, **60**, 13579–13586.

8 For selected reviews of azomethine ylides:(*a*) L. Wei, L. Xiao, Y. Z. Hu, Z. F. Wang, H. Y. Tao and C. J. Wang, *Chin. J. Org. Chem.*, 2019, **39**, 2119–2130; (*b*) L. Wei, X. Chang and C. J. Wang, *Acc. Chem. Res.*, 2020, **53**, 1084–1100; (*c*) L. Wei, X. Chang, Z. P. Zhang, Z. F. Wang and C. J. Wang, *Chin. Sci. Bull.*, 2023, **68**, 3956–3968.

9 For selected reviews on carbonyl catalysis:(*a*) Y. C. Luo, H. H. Zhang, Y. Wang and P. F. Xu, *Acc. Chem. Res.*, 2010, **43**, 1317–1330; (*b*) A. E. Sorochinsky, J. L. Aceña, H. Moriwaki, T. Sato and V. Soloshonok, *Amino Acids*, 2013, **45**, 1017–1033; (*c*) Q. Wang, Q. Gu and S. L. You, *Angew. Chem., Int. Ed.*, 2019, **58**, 6818–6825; (*d*) W. Wen and Q. X. Guo, *Synthesis*, 2023, **55**, 719–732; (*e*) X. Xiao and B. G. Zhao, *Acc. Chem. Res.*, 2023, **56**, 1097–1117For recent selected examples on asymmetric Aldol reaction:; (*f*) A. L. Cheng, L. L. Zhang, Q. H. Zhou, T. Liu, J. Cao, G. Q. Zhao, K. Zhang, G. S. Song and B. G. Zhao, *Angew. Chem., Int. Ed.*, 2021, **60**, 20166–20172; (*g*) P. W. Ji, X. P. Liu, J. W. Xu, X. Zhang, J. H. Guo, W. W. Chen and B. G. Zhao, *Angew. Chem., Int. Ed.*, 2022, **61**, e202206111; (*h*) C. K. Hou, B. F. Peng, S. Ye, Z. Y. Yin, J. Cao, X. Xiao and B. G. Zhao, *Nat. Catal.*, 2022, **5**, 1061–1068.

10 (*a*) C. K. Prier, D. A. Rankic and D. W. C. MacMillan, *Chem. Rev.*, 2013, **113**, 5322–5363; (*b*) J. R. Chen, X. Q. Hu, L. Q. Lu and W. J. Xiao, *Chem. Soc. Rev.*, 2016, **45**, 2044–2056.

11 For selected examples of excited ketones:(*a*) P. J. Wagner, *Chemistry of Excited Triplet Organic Carbonyl Compounds. Triplet States III; Topics in Current Chemistry*, Springer, vol. 66, 1976, pp. 1–52; (*b*) P. J. Wagner and R. A. Leavitt, *J. Am. Chem. Soc.*, 1973, **95**, 3669–3677; (*c*) P. J. Wagner, R. J. Truman, A. E. Puchalski and R. Wake, *J. Am. Chem. Soc.*, 1986, **108**, 7727–7738; (*d*) C. Chen, *Org. Biomol. Chem.*, 2016, **14**, 8641–8647; (*e*) M. Fréneau and N. Hoffmann, *J. Photochem. Photobiol., C*, 2017, **33**, 83–108; (*f*) Á. Péter, S. Agasti, O. Knowles, E. Pye and D. J. Procter,

Chem. Soc. Rev., 2021, **50**, 5349–5365; (*g*) H.-M. Huang, P. Bellotti and F. Glorius, *Acc. Chem. Res.*, 2022, **55**, 1135–1147; (*h*) X. B. Bai, J. L. Yao, W. X. Li, X. W. Zhao, Y. L. Yin, S. Y. Yu and Z. Y. Jiang, *Org. Lett.*, 2024, **26**, 5037–5042.

12 For selected reviews and examples on CLA–catalyzed photochemical reactions of aryl ketones:(*a*) L. L. Zhang and E. Meggers, *Acc. Chem. Res.*, 2017, **50**, 320–330; (*b*) X. Q. Huang and E. Meggers, *Acc. Chem. Res.*, 2019, **52**, 833–847; (*c*) L. Z. Hou, X. H. Liu, W. D. Cao and X. M. Feng, *ChemCatChem*, 2023, **15**, e202300893; (*d*) C. Y. Wang, J. Qin, X. D. Shen, R. Riedel, K. Harms and E. Meggers, *Angew. Chem., Int. Ed.*, 2016, **55**, 685–688; (*e*) J. J. Ma, A. R. Rosales, X. Q. Huang, K. Harms, R. Riedel, O. Wiest and E. Meggers, *J. Am. Chem. Soc.*, 2017, **139**, 17245–17248; (*f*) F. Y. Li, D. Tian, Y. F. Fan, R. Lee, G. Lu, Y. L. Yin, B. K. Qiao, X. W. Zhao, Z. W. Xiao and Z. Y. Jiang, *Nat. Commun.*, 2019, **10**, 1774; (*g*) Z. D. Tan, S. B. Zhu, Y. B. Liu and X. M. Feng, *Angew. Chem., Int. Ed.*, 2022, **61**, e202203374; (*h*) J. B. Kidd, T. A. Fiala, W. B. Swords, Y. Park, K. A. Meyer, K. M. Sanders, L. A. Guzei, J. C. Wright and T. P. Yoon, *J. Am. Chem. Soc.*, 2024, **146**, 15293–15300.

13 (*a*) X.-K. He, L.-Q. Lu, B.-R. Yuan, J.-L. Luo, Y. Cheng and W.-J. Xiao, *J. Am. Chem. Soc.*, 2024, **146**, 18892–18898; (*b*) Z. W. Zhong, H. D. Wu, X. F. Chen, Y. Luo, L. Q. Yang, X. M. Feng and X. H. Liu, *J. Am. Chem. Soc.*, 2024, **146**, 20401–20413.

14 L. Chang, Q. An, L. F. Duan, K. X. Feng and Z. W. Zuo, *Chem. Rev.*, 2022, **122**, 2429–2486.

15 For reviews on chiral *N,N′*-dioxides:(*a*) X. H. Liu, L. L. Lin and X. M. Feng, *Acc. Chem. Res.*, 2011, **44**, 574–587; (*b*) X. H. Liu, L. L. Lin and X. M. Feng, *Org. Chem. Front.*, 2014, **1**, 298–302; (*c*) X. H. Liu, H. F. Zheng, Y. Xia, L. L. Lin and X. M. Feng, *Acc. Chem. Res.*, 2017, **50**, 2621–2631; (*d*) X. H. Liu, S. X. Dong, L. L. Lin and X. M. Feng, *Chin. J. Chem.*, 2018, **36**, 791–797; (*e*) Z. Wang, X. H. Liu and X. M. Feng, *Aldrichim Acta*, 2020, **53**, 3–10; (*f*) L. L. Lin, Y. Q. Zhou, W. D. Cao, S. X. Dong, X. H. Liu and X. M. Feng, *Sci. China: Chem.*, 2023, **53**, 246–258; (*g*) S. X. Dong, W. D. Cao, M. P. Pu, X. H. Liu and X. M. Feng, *CCS Chem.*, 2023, **5**, 2717–2735; (*h*) G. H. Pan, C. L. He, M. Chen, Q. Xiong, W. D. Cao and X. M. Feng, *CCS Chem.*, 2022, **4**, 2000–2008; (*i*) Z. W. Zhong, L. C. Ning, Y. C. Lu, J. Q. Tan, L. L. Lin and X. M. Feng, *Sci. China: Chem.*, 2023, **66**, 799–807.

16 For selected examples on photocatalytic reactions with chiral *N,N′*-dioxides:(*a*) H. Yu, S. X. Dong, Q. Yao, L. Chen, D. Zhang, X. H. Liu and X. M. Feng, *Chem.–Eur. J.*, 2018, **24**, 19361–19367; (*b*) L. K. Yang, W. Y. R. Li, H. L. Hou, T. Y. Zhan, W. D. Cao, X. H. Liu and X. M. Feng, *Chem. Sci.*, 2022, **13**, 8576–8582; (*c*) H. Yu, T. Y. Zhan, Y. Q. Zhou, L. Chen, X. H. Liu and X. M. Feng, *ACS Catal.*, 2022, **12**, 5136–5144; (*d*) L. Z. Hou, Y. Q. Zhou, H. Yu, T. Y. Zhan, W. D. Cao and X. M. Feng, *J. Am. Chem. Soc.*, 2022, **144**, 22140–22149; (*e*) Y. Luo, Q. Wei, L. K. Yang, Y. Q. Zhou, W. D. Cao, Z. S. Su, X. H. Liu and X. M. Feng, *ACS Catal.*, 2022, **12**, 12984–12992; (*f*) L. L. Feng, X. F. Chen, N. Guo,

Y. Q. Zhou, L. L. Lin, W. D. Cao and X. M. Feng, *Chem. Sci.*, 2023, **14**, 4516–4522; (*g*) T. Y. Zhan, L. K. Yang, Q. Y. Chen, R. Weng, X. H. Liu and X. M. Feng, *CCS Chem.*, 2023, **5**, 2101–2110; (*h*) L. K. Yang, L. C. Ning, H. Yu, S. Y. Li, M. Yang, L. H. Yang, F. Wang, X. H. Liu, W. D. Cao and X. M. Feng, *CCS Chem.*, 2024, DOI: 10.31635/ccschem.024.202404257; (*i*) L. Z. Hou, L. Q. Yang, G. F. Yang, Z. Luo, W. L. Xiao, L. H. Yang, F. Wang, L.-Z. Gong, X. H. Liu, W. D. Cao and X. M. Feng, *J. Am. Chem. Soc.*, 2024, **146**, 23457–23466; (*j*) Y. Luo, Y. Q. Zhou, F. N. Xiao, X. He, Z. W. Zhong, Q.-L. Zhou, W. D. Cao, X. H. Liu and X. M. Feng, *ACS Catal.*, 2024, **14**, 12031–12041.

17 CCDC 2320632 for **C5** contains the supplentary crystallographic data for this paper. These data are provided free of charge by the joint Cambridge Crystallographic Data Centre and Fachinformationszentrum Karlsruhe Access Structures service.

18 For selected examples for application of 2-amino-1,3-diols:(*a*) M. P. Sibi, J. X. Chen and G. R. Cook, *Tetrahedron Lett.*, 1999, **40**, 3301–3304; (*b*) J. V. Allen and J. M. J. Williams, *Tetrahedron: Asymmetry*, 1994, **5**, 277–282.

19 M. J. Frisch, G. W. Trucks, H. B. Schlegel, G. E. Scuseria, M. A. J. R. Robb, J. R. Cheeseman, G. Scalmani, V. Barone, B. Mennucci, G. A. Petersson, H. Nakatsuji, M. Caricato, X. Li, H. P. Hratchian, A. F. Izmaylov, J. Bloino, G. Zheng, J. L. Sonnenberg, M. Hada, M. Ehara, K. Toyota, R. Fukuda, J. Hasegawa, M. Ishida, T. Nakajima, Y. Honda, O. Kitao, H. Nakai, T. Vreven, J. A. Montgomery Jr, J. E. Peralta, F. Ogliaro, M. Bearpark, J. J. Heyd, E. Brothers, K. N. Kudin, V. N. Staroverov, R. Kobayashi, J. Normand, K. Raghavachari, A. Rendell, J. C. Burant, S. S. Iyengar, J. Tomasi, M. Cossi, N. Rega, M. J. Millam, M. Klene, J. E. Knox, J. B. Cross, V. Bakken, C. Adamo, J. Jaramillo, R. Gomperts, R. E. Stratmann, O. Yazyev, A. J. Austin, R. Cammi, C. Pomelli, J. W. Ochterski, R. L. Martin, K. Morokuma, V. G. Zakrzewski, G. A. Voth, P. Salvador, J. J. Dannenberg, S. Dapprich, A. D. Daniels, Ö. Farkas, J. B. Foresman, J. V. Ortiz, J. Cioslowski and D. J. Fox, *Gaussian09, Revision D.01*, Gaussian, Inc., Wallingford, CT, 2013.

20 (*a*) T. Lu and F. W. Chen, *J. Comput. Chem.*, 2012, **33**, 580–592; (*b*) T. Lu and Q. X. Chen, *J. Comput. Chem.*, 2022, **43**, 539–555.